FUNCTIONALIZATION OF COTTON FABRIC WITH POLYANILINE EMERALDINE SALT USING SILANE ANILINE AS COUPLING AGENT

JAMES VINCENT D.V. ANG,[*] ALVIN KARLO G. TAPIA,[*] CHRYSLINE MARGUS N. PIÑOL,[*] NACITA B. LANTICAN,[**] MA. LOURDES F. DEL MUNDO,[**] RONNIEL D. MANALO[***] and MARVIN U. HERRERA[*]

[*] *Institute of Physics, College of Arts and Sciences, University of the Philippines Los Baños, Laguna, 4031, Philippines*
[**] *Institute of Biological Sciences, College of Arts and Sciences, University of the Philippines Los Baños, Laguna, 4031, Philippines*
[***] *Department of Forest Products and Paper Science, College of Forestry and Natural Resources, University of the Philippines Los Baños, Laguna, 4031, Philippines*
✉ *Corresponding author: A. K. G. Tapia, agtapia@up.edu.ph*

Received April 27, 2025

Silane-aniline coupling agents were employed to attach polyaniline emeraldine salt (PAni-ES) to cotton fabrics. The cellulose fibers of the cotton fabric were functionalized with silane-aniline molecules using a simple soaking technique. Oxidative polymerization was carried out to form polyaniline molecules from the attached aniline groups. The structural characteristics of the PAni-ES functionalized cotton were analyzed using Fourier Transform Infrared (FTIR) Spectroscopy and Time-of-Flight Secondary Ion Mass Spectroscopy (ToF-SIMS). FTIR spectra revealed peaks corresponding to the polyaniline structure, suggesting successful attachment. ToF-SIMS showed prominent signals (~10^{-2}) for $SiC_2H_5O^+$ (73.02 u) and $Si_3C_4HN^+$ (146.91 u). This indicates strong bonding between the silane-aniline molecules and the polyaniline. The functionalized PAni-ES cotton samples exhibited enhanced antimicrobial properties against *Staphylococcus aureus* (gram-positive) and *Escherichia coli* (gram-negative), demonstrating the effectiveness of the functionalization approach.

Keywords: antimicrobial, ToF-SIMS, FTIR, organosilane, polyaniline

INTRODUCTION

Cotton-based fabrics, primarily composed of cellulosic materials, are characterized by their low density, fibrous structure, and flexibility. These properties make them suitable for a wide range of applications, such as in textile manufacturing, hygiene and sanitation materials, and biomedical fields. The integration of functional materials[1-10] onto cotton fabrics can substantially enhance their utility, expanding their potential use to include flexible electronics, electromagnetic (EM) shielding, and antimicrobial textiles. Such functional modifications not only improve the material's applicability, but also increase its commercial value and market competitiveness.

Various materials are incorporated into cellulose-based fabrics/textiles through different techniques to enhance their functionality for specific applications. However, fabrics are often subjected to multiple aging conditions, such as rubbing and washing, which can lead to the removal of incorporated materials. This issue of leachability is particularly relevant for textiles functionalized with materials that are weakly bound to the cellulose fibers.

One potential strategy to reduce leachability is to create stronger chemical bonds between the cellulose and the functional material. This can be achieved through the use of a coupling agent or linker, which establishes a chemical bridge between the cellulose and the functional material. Organosilane molecules are commonly used coupling agents. They possess two selectively reactive ends. One end is reactive on a particular surface, while the other end is not. This property allows organosilane molecules to self-assemble into molecular layers, with the surface-reactive ends oriented toward the substrate and the surface-inert ends oriented outward. The surface-inert end

can subsequently be functionalized for other purposes. Silane-based materials[11-15] have been successfully attached or grafted to a wide variety of substrates, demonstrating their versatility in materials processing.

This study further explores the potential of silane-aniline as a coupling agent. The surface-reactive end contains three hydrolyzed groups, which are expected to interact with the hydroxyl groups of cellulose, while the surface-inert end is pre-functionalized with an aniline group. The aniline group serves as a site for the polymerization of aniline monomers into polyaniline molecules. Polyaniline[16-23] is an intrinsically conductive polymer and has good stability. It is also easy to synthesize and produce from a relatively economical monomer. Additionally, polyaniline has redox-active carbon-nitrogen bonds, which have potential antimicrobial properties.[24-30]

EXPERIMENTAL

Chemical reagents used

The following chemical reagents were used without further purification: N-[3-(trimethoxysilyl) propyl] aniline (Aldrich), absolute ethanol (Ajax Finechem), aniline (Sigma Aldrich, >99.5%), HCl (37% ACI-Labscan), and ammonium persulfate (APS).

Pretreatment and functionalization via soaking

Commercially available 100% cotton fabric (Hanes®) was cut into 4 cm x 3 cm pieces. The cotton fabric was immersed in absolute ethanol and sonicated for 15 minutes. After sonication, the cotton sample was air dried under ambient conditions.

Functionalization was done by immersing the cotton fabric in 40 mL of 2% v/v silane aniline-ethanol solution for 24 hours. The silane aniline-ethanol solution was prepared by mixing N-[3-(trimethoxysilyl)propyl] aniline (silane aniline) and absolute ethanol. Absolute ethanol was used to minimize the self-condensation of silane aniline with each other. After functionalization, the samples were dried inside a furnace for one hour at 80 °C.

Oxidative polymerization of functionalized cotton

The functionalized cotton samples were soaked in a 0.8 HCl-aniline solution for 30 minutes inside a Petri dish. The wet samples were then transferred to another Petri dish. After this, 0.25 APS solution was gradually added. The samples were immersed in APS solution for 30 minutes before they were dried in a furnace for one hour at 60 °C.

To remove the loosely adhered materials, the samples were sonicated in ethanol for 15 minutes, then in water for another 15 minutes, then again in ethanol for 15 minutes. The samples were then air-dried.

Characterization

The infrared spectrum was obtained using a Perkin Elmer Frontier Fourier Transform Infrared (FTIR) Spectrometer in Attenuated Total Reflectance (ATR) Mode. The range of scanning was between 4000-600 cm^{-1}. Relative (Rel.) transmittance was calculated as follows:

$$Rel.Transmittance = \frac{T_{sample} - T_{reference}}{T_{reference}} \quad (1)$$

where T_{sample} corresponds to the FTIR spectrum of the sample, while $T_{reference}$ corresponds to the FTIR spectrum of the untreated cotton fabric.

The secondary ion mass spectrum was obtained using an ION TOF TOF-SIMS 5, a time-of-flight secondary ion mass spectrometer (TOF-SIMS). The UV-visible spectrum was obtained using a Shimadzu UV-Visible Spectrometer (UV-2600), with an integrating sphere attachment (ISR-2600Plus), to facilitate the detection of reflected light signals.

The antimicrobial properties of the functionalized cotton fabric against *Staphylococcus aureus* (gram-positive) and *Escherichia coli* (gram-negative) bacteria were tested under dynamic contact conditions (ASTM E2149-01).

RESULTS AND DISCUSSION

Figure 1 presents the infrared (IR) spectrum of the cotton fabric following silane-aniline functionalization and subsequent oxidative polymerization. Figures 2 and 3 show the secondary ion mass and the reflectance spectra, respectively, of the cotton fabric after oxidative polymerization. Tables 1, 2 and 3 provide a summary of the key peaks observed in these spectra and their corresponding interpretations. The coupling agent used in this study is a silane-aniline molecule, whose molecular structure is shown in Figure 4. Schematic models illustrating the proposed molecular configurations are shown in Figure 5 for the fabric after silane-aniline functionalization, and in Figure 6 following oxidative polymerization.

Silane-aniline consists of a surface-reactive end (three OCH_3 groups), a surface-inert end (aniline), and a hydrocarbon backbone, as illustrated in Figure 4. During the functionalization process, the reactive end reacts with the hydroxyl groups of cellulose, forming Si-O bonds. These bonds are manifested by the presence of Si-O stretching in the IR spectra at 1084 cm^{-1}. On the other hand, the aniline group, which serves both as the surface-inert group and as the functional group, is oriented away from the cellulose surface in Figure 5. The IR spectrum reveals two types of aromatic rings: benzenoid rings at 1508 cm^{-1} and quinoid rings at 1604 cm^{-1}. The benzenoid ring in Figure 5 (a) is the

original form of the aromatic ring present in the silane-aniline precursor. The appearance of some quinoid rings in Figure 5 (b-d) suggests partial transformation, which may have been caused by charge delocalization during grafting or by an internal redox process.

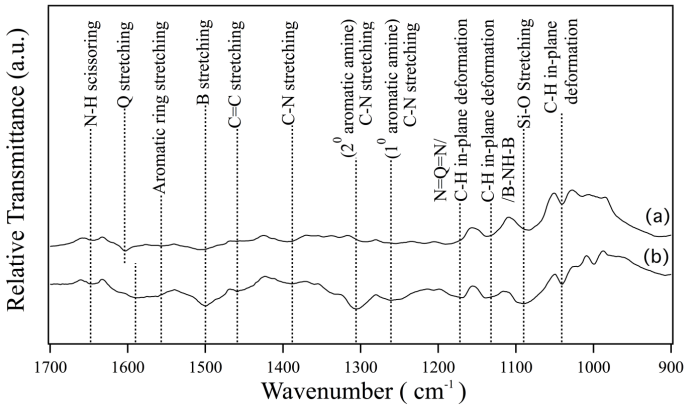

Figure 1: Infrared spectra of cotton fabric after (a) silane aniline functionalization, and (b) oxidative polyaniline polymerization – the infrared spectrum of a cotton fabric was used as reference for calculating the relative transmittance (Note: "Q" stands for "quinoid ring", "B" – "benzenoid ring", "1°" – "primary" and "2°" – "secondary")

Table 1
Peaks of infrared spectra presented in Figure 1 (a and b) and their corresponding interpretation

Wavenumber (cm^{-1})		Interpretation
(a)	(b)	
1648	1648	N-H scissoring
1604	1590	Quinoid (Q) ring stretching
1557	1562	Aromatic ring stretching
1508	1500	Benzenoid (B) ring stretching
1458	1459	C=C stretching in aromatic ring
1393	1388	C-N stretching
	1306	C-N stretching (secondary aromatic amine)
	1261	C-N stretching (primary aromatic amine)
	1172	N=Q=N / C-H in-plane deformation
1137	1132	C-H in-plane deformation / B-NH-B
1084	1090	Si-O stretching
1041	1041	C-H in-plane deformation

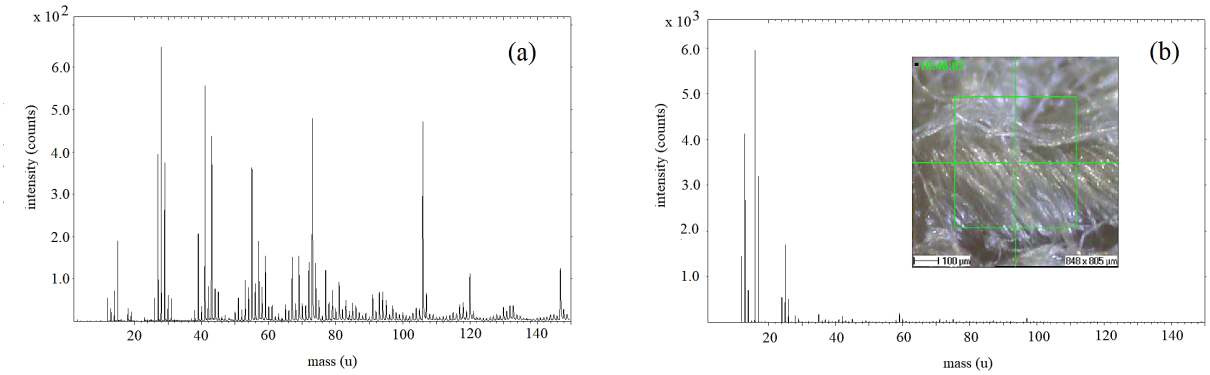

Figure 2: (a) Positive and (b) negative ions secondary ion mass spectra of a cotton fabric after silane aniline functionalization and oxidative polyaniline polymerization (inset: region wherein the data were collected)

Table 2
Peaks of positive and negative ions secondary ion mass spectra of the sample presented in Figure 2 (peak area is normalized with respect to the total ion intensity)

Positive ions			Negative ions		
Mass (u)	Peak area	Interpretation	Mass (u)	Peak area	Interpretation
12.01	1.57×10^{-03}	C^+	12.00	2.66×10^{-02}	C^-
13.02	1.23×10^{-03}	CH^+	13.01	6.61×10^{-02}	CH^-
14.04	2.51×10^{-03}	CH_2^+	14.02	1.04×10^{-02}	CH_2^-
15.05	5.72×10^{-03}	CH_3^+	15.03	5.53×10^{-04}	CH_3^-
18.06	9.36×10^{-04}	NH_4^+	15.99	1.11×10^{-01}	O^-
19.04	5.47×10^{-04}	F^+	17.00	5.58×10^{-02}	OH^-
23.01	2.45×10^{-04}	Na^+	19.01	1.87×10^{-04}	F^-
26.03	1.99×10^{-03}	$C_2H_2^+$	24.00	1.01×10^{-02}	C_2^-
27.04	1.60×10^{-02}	$C_2H_3^+$	25.01	3.12×10^{-02}	C_2H^-
27.98	3.45×10^{-02}	Si^+	26.01	1.00×10^{-02}	CN^-
28.04	3.27×10^{-03}	$C_2H_4^+$	27.98	3.22×10^{-03}	Si^-
28.99	9.45×10^{-03}	SiH^+	28.99	1.96×10^{-03}	SiH^-
29.05	1.55×10^{-02}	$C_2H_5^+$	31.99	6.23×10^{-04}	O_2^-
29.97	1.58×10^{-03}	$^{30}Si^+$	34.97	3.76×10^{-03}	Cl^-
30.05	2.66×10^{-03}	$C_2H_6^+$	36.97	1.13×10^{-03}	$^{37}Cl^-$
31.03	2.32×10^{-03}	$N_2H_3^+$	41.01	1.87×10^{-03}	C_2HO^-
38.01	7.82×10^{-04}	CH_3Na^+	42.01	3.35×10^{-03}	$C_2H_2O^-$
39.02	9.95×10^{-03}	$C_3H_3^+$	43.99	5.37×10^{-04}	SiO^-
41.04	2.93×10^{-02}	$C_3H_5^+$	45.01	1.98×10^{-03}	$C_2H_2F^-$
42.04	4.30×10^{-03}	$C_2H_4N^+$	49.02	8.48×10^{-04}	$CH_5O_2^-$
42.99	2.47×10^{-02}	C_2F^+	58.02	1.45×10^{-03}	$CH_2N_2O^-$
43.06	2.68×10^{-02}	$C_3H_7^+$	59.03	6.05×10^{-03}	$CH_3N_2O^-$
44.00	4.14×10^{-03}	SiO^+	59.98	2.10×10^{-03}	SiO_2^-
44.05	4.56×10^{-03}	$C_2H_6N^+$	71.04	1.97×10^{-03}	$C_4H_4F^-$
44.97	1.82×10^{-03}	$SiHO^+$	73.03	1.44×10^{-03}	$CH_4F_3^-$
45.03	5.14×10^{-03}	CH_3NO^+	75.02	2.11×10^{-03}	$C_6H_3^-$
53.02	5.08×10^{-03}	$C_3H_3N^+$	97.01	3.48×10^{-03}	$C_3HN_2O_2^-$
54.02	4.28×10^{-03}	$C_2H_2N_2^+$			
55.04	2.71×10^{-02}	$C_3H_5N^+$			
56.04	5.69×10^{-03}	$C_2H_4N_2^+$			
57.05	1.70×10^{-02}	$C_3H_5O^+$			
58.05	4.81×10^{-03}	$C_2H_6N_2^+$			
59.02	1.12×10^{-02}	$SiCH_5N^+$			
60.01	2.23×10^{-03}	SiO_2^+			
67.02	1.07×10^{-02}	$C_4H_3O^+$			
69.03	1.42×10^{-02}	$C_4H_5O^+$			
72.01	1.17×10^{-02}	$SiCH_4N_2^+$			
73.02	4.91×10^{-02}	$SiC_2H_5O^+$			
74.01	1.01×10^{-02}	$C_6H_2^+$			
76.99	9.71×10^{-03}	$Si_2H_5O^+$			
79.01	6.04×10^{-03}	$C_5H_3O^+$			
81.01	7.61×10^{-03}	$SiC_3H_3N^+$			
105.96	4.32×10^{-02}	$CO_3Na_2^+$			
119.96	1.16×10^{-02}	$Si_2C_5H_4^+$			
146.91	1.40×10^{-02}	$Si_3C_4HN^+$			

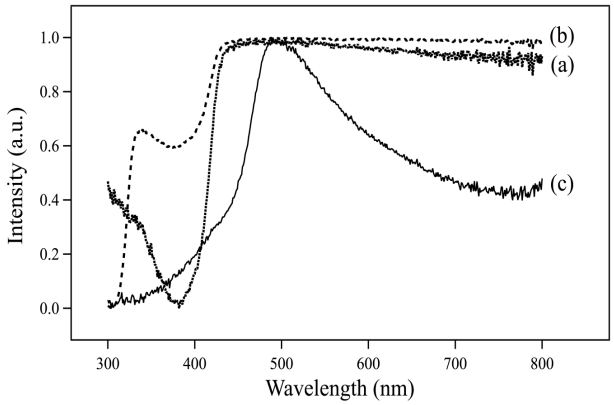

Figure 3: Reflectance spectrum of (a) initial cotton fabric, (b) silane aniline-functionalized cotton fabric, and (c) polyaniline-functionalized cotton fabric in ultraviolet and visible light regions

During oxidative polymerization, the grafted silane molecules serve as sites for polyaniline polymerization, as presented in Figure 6. The associated IR spectrum continues to show Si-O stretching (1900 cm^{-1}), indicating that the coupling agents are still intact on the cellulose surface. The presence of quinoid ring stretching (1590 cm^{-1}) and benzenoid ring stretching (1500 cm^{-1}) are expected since they are the building blocks of polyaniline molecules. Additionally, the peaks observed at 1306 cm^{-1} and 1172 cm^{-1} are attributed to the secondary aromatic amine and N=Q=N structure, respectively. Secondary aromatic amines are located between benzenoid rings, while the N=Q=N structure (containing a central C=N bond) is found between the benzenoid and quinoid rings. Notably, the peaks associated with the stretching of quinoid and aromatic rings become broader.

Time-of-Flight Secondary Ion Mass Spectroscopy (ToF-SIMS) detects the presence of ionic fragments containing carbon, hydrogen and nitrogen atoms, such as $C_2H_4N^+$ (42.04 u), $C_2H_6N^+$ (44.05 u), $C_3H_3N^+$ (53.02 u), $C_2H_2N_2^+$ (54.02 u), $C_3H_5N^+$ (55.04 u), $C_2H_4N_2^+$ (56.04 u), $C_2H_6N_2^+$ (58.05 u). This supports the presence of polyaniline molecules in the samples. It is important to note that the sample exhibits a distinct green color, which is also observed in the reflectance spectra of the polyaniline-functionalized sample in Figure 3. This feature is characteristic of protonated polyaniline molecules or polyaniline emeraldine salt. This is expected since the aniline monomers, which were used, are in an acidic medium, hydrochloric acid.

A silicon atom has four valence electrons, which allows it to form up to four covalent bonds with surrounding atoms. In the functionalized cotton, silicon acts as a bridge linking cellulose substrate with grafted polyaniline molecules. Insights into these linkages are provided by the ToF-SIMS, which reveals several silicon-containing ionic fragments. Fragments such as $SiCH_5N^+$ (59.02 u), $SiCH_4N_2^+$ (72.01 u), $SiC_3H_3N^+$ (81.01 u) suggest that at least one of the valence electrons of the silicon atom is attached to a carbon atom of polyaniline molecule or a carbon atom that holds the polyaniline molecules, as in Figure 6 (a).

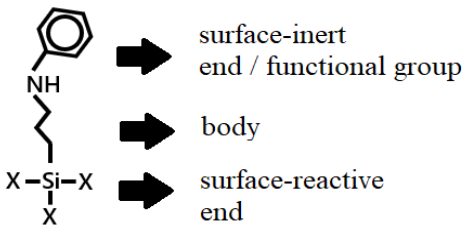

Figure 4: Molecular structure of silane aniline molecules (X stands for OCH_3)

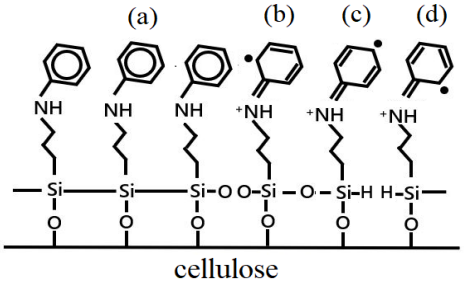

Figure 5: Proposed model of the configuration of silane aniline molecules after functionalization: (a) benzenoid rings and (b-d) quinoid rings

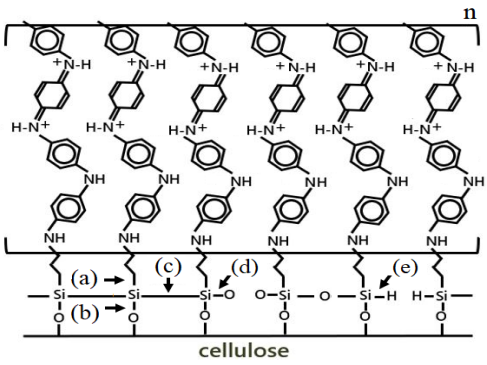

Figure 6: Proposed configuration of molecules attached after oxidative polymerization of functionalized cotton (Cl counter ions are not shown)

Table 4
Antimicrobial property of samples against *E. coli* and *S. aureus*

Samples	Reduction (%)	
	E. coli	*S. aureus*
Cotton fabric	49 ± 1	55 ± 5
Cotton fabric after silane functionalization	64 ± 3	81 ± 2
Cotton fabric after oxidative polymerization	74 ± 3	85 ± 1

Fragments containing silicon and oxygen atoms, such as $SiC_2H_5O^+$ (73.02u), SiO^+ (44.00 u), SiO^- (43.99u), indicate that another valence electron of the silicon atom forms a bond with the hydroxyl group of cellulose, establishing Si-O linkages, as shown in Figure 6 (b). This is further supported by the IR spectrum, which exhibits Si-O bonds at 1900 cm^{-1}, and by the relatively high peak associated with $SiC_2H_5O^+$ in the ToF-SIMS data (~10^{-2}).

The remaining two valence electrons of the silicon atom influence possible interactions and bonding among the grafted silane molecules. The presence of ionic fragments containing multiple silicon atoms, such as $Si_3C_4HN^+$ (146.91 u), $Si_2C_5H_4^+$ (119.96 u) suggests the potential formation of Si-Si bonds between neighboring silane molecules shown in Figure 6 (c). The relatively high intensities of these fragments (~10^{-2}) support the predominance of Si-Si structures. In addition to the Si-Si bonding, the presence of ionic fragments with silicon and two oxygen atoms, such as SiO_2^+ (60.01 u) and SiO_2^- (59.98 u), is also possible, as in Figure 6 (d). However, the intensities of the mentioned ionic fragments are relatively low (~10^{-3}). Aside from oxygen, the attached atom on the lateral side could also be hydrogen, as in Figure 6 (e). ToF-SIMS analysis supports this with the identification of SiH^+ (28.99 u), SiH^- (28.99 u), and $SiHO^+$ (44.97 u).

Table 4 presents the antimicrobial activity of the cotton fabrics against *E. coli* and *S. aureus* following functionalization with silane-aniline and oxidative polymerization. After the silane-aniline treatment, the bacterial reduction efficiency increased to 64% ± 3% for *E. coli* and 81% ± 2% for *S. aureus*. This antimicrobial performance was further enhanced after oxidative polymerization, reaching 74% ± 3% and 85% ± 1% for *E. coli* and *S. aureus*, respectively. The improved antimicrobial properties of the treated cotton fabric are attributed to the presence of the amine group. Amines are redox-active. Thus, they can directly or indirectly disrupt charge transport within the cell. Such disruption can impair vital cellular processes, ultimately leading to inhibition or cell death.

The functionalized fabrics exhibit stronger antimicrobial activity against *S. aureus* (gram-positive), compared to *E. coli* (gram-negative). This enhanced efficacy towards *S. aureus* is likely due to the porous nature of its cell wall, which makes it more vulnerable to external agents. In contrast, *E. coli* possesses a more complex outer membrane composed of phospholipids, lipoproteins, and lipopolysaccharide, which serve as a protective barrier against external threats, reducing the fabric's antimicrobial effectiveness.

CONCLUSION

Polyaniline emeraldine salt was successfully grafted onto cotton fabrics using silane-aniline as the coupling agent. The functionalization process involved a simple soaking method to anchor silane-aniline molecules onto the cellulose fibers, followed by oxidative polymerization to grow polyaniline molecules from the attached sites. FTIR spectroscopy confirmed the presence of characteristic vibrational bands associated with the molecular moieties of polyaniline, ToF-SIMS analysis revealed key ionic fragments produced upon surface bombardment, offering insights into the chemical structure of the modified fabric. The combined observations from FTIR and ToF-SIMS enabled the development of a proposed model describing the architecture of the grafted system. Notably, the strong ToF-SIMS signals ($\sim 10^{-2}$) coming from $SiC_2H_5O^+$ (73.02 u) and $Si_3C_4HN^+$ (146.91 u) suggest that the silicon atoms are bonded to cellulose fibers and to neighboring silane molecules, forming a stable interlinked network. Furthermore, both silane-aniline-functionalized and polyaniline-functionalized cotton samples demonstrated enhanced microbial activity, particularly against *Staphylococcus aureus* (gram-positive) compared to *Escherichia coli* (gram-negative).

In-situ oxidative polymerization of functionalized polyaniline on cotton typically preserves the cellulose structure, provided the reaction avoids harsh conditions, such as strong acids, excessive oxidant concentrations, elevated temperatures, or prolonged reaction times. Nevertheless, further evaluation of the material's breathability and mechanical durability is required to assess its suitability for wearable device applications.

ACKNOWLEDGEMENT: This research is funded by the Philippine Council for Industry, Energy, and Emerging Technology Research and Development (PCIEERD) with project number 04013.

REFERENCES

[1] P. Gahlout and V. Choudhary, *Compos. B Eng.*, **175**, 107093 (2019), https://doi.org/10.1016/j.compositesb.2019.107093

[2] T. T. Hanh, N. T. Thu, N. Q. Hien, P. N. An, T. T. K. Loan *et al.*, *Radiat. Phys. Chem.*, **121**, 87 (2016), http://dx.doi.org/10.1016/j.radphyschem.2015.12.024

[3] Shahid-ul-Islam, B. S. Butola and D. Verma, *Int. J. Biol. Macromol.*, **133**, 1134 (2019), https://doi.org/10.1016/j.ijbiomac.2019.04.186

[4] N. Marakova, P. Humpolicek, V. Kasparkova, Z. Capakova, L. Martinkova *et al.*, *Appl. Surf. Sci.*, **396**, 169 (2017), http://dx.doi.org/10.1016/j.apsusc.2016.11.024

[5] S. Mura, G. Greppi, L. Malfatti, B. Lasio, V. Sanna *et al.*, *J. Colloid Interface Sci.*, **456**, 85 (2015), http://dx.doi.org/10.1016/j.jcis.2015.06.018

[6] R. Pandimurugan and S. Thambidurai, *Int. J. Biol. Macromol.*, **105**, 788 (2017), http://dx.doi.org/10.1016/j.ijbiomac.2017.07.097

[7] R. Rajendran, R. Radhai, T. M. Kotresh and E. Csiszar, *Carbohyd. Polym.*, **91**, 613 (2013), http://dx.doi.org/10.1016/j.carbpol.2012.08.064

[8] Th. I. Shaheen and A. A. A. El Aty, *Int. J. Biol. Macromol.*, **118**, 2121 (2018), https://doi.org/10.1016/j.ijbiomac.2018.07.062

[9] P. Sharma, S. Pant, V. Dave, K. Tak, V. Sadhu *et al.*, *J. Microbiol. Methods*, **160**, 107 (2019), https://doi.org/10.1016/j.mimet.2019.03.007

[10] M. Shateri-Khalilabad, M. E. Yazdanshenas and A. Etemadifar, *Arab. J. Chem.*, **10**, S2355 (2017), http://dx.doi.org/10.1016/j.arabjc.2013.08.013

[11] L. Fang, L. Chang, W. Guo, Y. Chen and Z. Wang, *Appl. Surf. Sci.*, **288**, 682 (2014), http://dx.doi.org/10.1016/j.apsusc.2013.10.098

[12] M. Sabzi, S. M. Mirabedini, J. Zohuriaan-Mehr and M. Atai, *Prog. Org. Coat.*, **65**, 222 (2009), https://doi.org/10.1016/j.porgcoat.2008.11.006

[13] Y. Xie, C. A. S. Hill, Z. Xiao, H. Militz and C. Mai, *Compos. A Appl. Sci.*, **41**, 806 (2010), https://doi.org/10.1016/j.compositesa.2010.03.005

[14] C.-H. Xue, Q.-Q. Fan, X.-J. Guo, Q.-F. An and S.-T. Jia, *Appl. Surf. Sci.*, **465**, 241 (2019), https://doi.org/10.1016/j.apsusc.2018.09.156

[15] J. Zhao, M. Milanova, M. C. G. Warmoeskerken and V. Dutschk, *Colloids Surf., A*, **413**, 273 (2012), https://doi.org/10.1016/j.colsurfa.2011.11.033

[16] S. Bhadra, D. Khastgir, N. K. Singha and J. H. Lee, *Prog. Polym. Sci.*, **34**, 783 (2009), https://doi.org/10.1016/j.progpolymsci.2009.04.003

[17] G. Ciric-Marjanovic, *Synth. Met.*, **177**, 1 (2013), http://dx.doi.org/10.1016/j.synthmet.2013.06.004

[18] N. Gospodinova and L. Terlemezyan, *Prog. Polym. Sci.*, **23**, 1443 (1998), https://doi.org/10.1016/S0079-6700(98)00008-2

[19] P. Humpolicek, V. Kasparkova, P. Saha and J. Stejskal, *Synth. Met.*, **162**, 722 (2012), https://doi.org/10.1016/j.synthmet.2012.02.024

[20] G. Liao, Q. Li and Z. Xu, *Prog. Org. Coat.*, **126**, 35 (2019), https://doi.org/10.1016/j.porgcoat.2018.10.018

[21] A. Pud, N. Ogurtsov, A. Korzhenko and G. Shapoval, *Prog. Polym. Sci.*, **28**, 1701 (2003), https://doi.org/10.1016/j.progpolymsci.2003.08.001

[22] J. Stejskal and R. G. Gilbert, *Pure Appl. Chem.*, **74**, 857 (2006), http://dx.doi.org/10.1351/pac200274050857

[23] M. Trchová and J. Stejskal, *Pure Appl. Chem.*, **83**, 1803 (2011), https://doi.org/10.1351/pac-rep-10-02-01
[24] A. N. Andriianova, L. R. Latypova, L. Y. Vasilova, S. V. Kiseleva, V. V. Zorin *et al.*, *J. Appl. Polym. Sci.*, **138**, 51397 (2021), https://doi.org/10.1002/app.51397
[25] A. Dolatkhah, P. R. Gupta, B. G. Steiger, M. Kazem-Rostami, M. Khani *et al.*, *Macromol. Chem. Phys.*, **2025**, e00335 (2025), https://doi.org/10.1002/macp.202500335
[26] M. Maruthapandi, A. Saravanan, A. Gupta, J. H. Luong and A. Gedanken, Macromolecules, **2**, 78 (2022), https://doi.org/10.3390/macromol2010005
[27] J. Robertson, M. Gizdavic-Nikolaidis, M. K. Nieuwoudt and S. Swift, *PeerJ*, **6**, e5135 (2018), https://doi.org/10.7717/peerj.5135
[28] M. R. Gizdavic-Nikolaidis, J. R. Bennett, S. Swift, A. J. Easteal and M. Ambrose, *Acta Biomater.*, **7**, 4204 (2011), https://doi.org/10.1016/j.actbio.2011.07.018
[29] N. Y. Abu-Thabit and A. S. H. Makhlouf, in "Industrial Applications for Intelligent Polymers and Coatings", edited by M. Hosseini and A. Makhlouf, Springer, Cham, 2016, pp. 437–477, https://doi.org/10.1007/978-3-319-26893-4_21
[30] E. N. Zare, P. Makvandi, B. Ashtari, F. Rossi, A. Motahari *et al.*, *J. Med. Chem.*, **63**, 1 (2019), https://doi.org/10.1021/acs.jmedchem.9b00803